



## Review

# Perspective of electrospun nanofibers in energy and environment

Jayaraman Sundaramurthy<sup>1,2\*</sup>, Ning Li<sup>1</sup>, P Suresh Kumar<sup>2</sup>, Seeram Ramakrishna<sup>1,2\*</sup>

<sup>1</sup>Center for Nanofibers and Nanotechnology, Department of Mechanical Engineering, National University of Singapore, Singapore 117576.

<sup>2</sup>Environmental & Water Technology, Centre of Innovation, Ngee Ann Polytechnic, Singapore

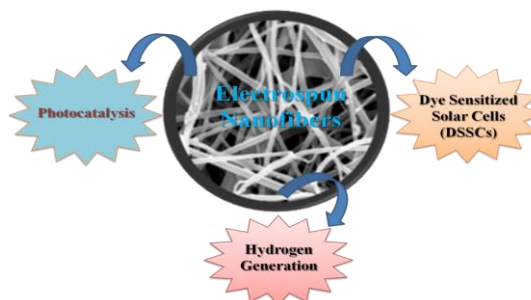
### HIGHLIGHTS

>Electrospinning is a simple, continuous and scalable technique to produce polymer composite and metal oxide nanofibers with high-aspect ratio and controlled morphologies.

>It possesses the added advantage of synthesizing porous, hollow and core/shell nanofibers with combination of additional polymers, metals and metal oxides for potential applications.

>This review focusses on the impact and role of electrospun nanofibers in improving the performances of DSSCs, photocatalysis and hydrogen generation & storage.

### GRAPHICAL ABSTRACT



### ARTICLE INFO

#### Article history:

Received 2 January 2014

Received in revised form 15 February 2014

Accepted 17 February 2014

Available online 26 April 2014

#### Keywords:

Electrospinning

Metal oxides

Nanostructures

Dye-sensitized solar cells

Photocatalysis and hydrogen storage

### ABSTRACT

This review summarizes the recent developments of electrospun semiconducting metal oxide/polymer composite nanostructures in energy and environment related applications. Electrospinning technique has the advantage of synthesizing nanostructures with larger surface to volume ratio, higher crystallinity with phase purity and tunable morphologies like nanofibers, nanowires, nanoflowers and nanorods. The electrospun nanostructures have exhibited unique electrical, optical and catalytic properties than the bulk counter parts as well as nanomaterials synthesized through other approaches. These nanostructures have improved diffusion and interaction of molecules, transfer of electrons along the matrix and catalytic properties with further surface modification and functionalization with combination of metals and metal oxides.

©2014 BRTeam CC BY 4.0

## 1. Introduction

In recent years, there has been an increasing need to meet the demands of power generation, consumption and storage using renewable energy sources while at the same time addressing the environmental pollutions by effective approaches (Arico et al., 2005, Fujishima et al., 2007). Researchers have been exploring different alternatives to address the issues using cheaper, eco-friendly and efficient nanomaterials (Guo, 2012). These materials possess large surface to volume ratio with controlled size and shape, which induce the possible new quantum mechanical effects than their bulk counter parts (Law

et al., 2004). Among the nanomaterials, semiconducting metal oxide/polymer composite nanostructures open up a new era in developing advanced functional materials and have the ability to generate power and be used for storage, as well as treating the effluents effectively (Kumar et al., 2012, Sahay et al., 2012). Metal oxides such as TiO<sub>2</sub>, ZnO, Fe<sub>2</sub>O<sub>3</sub>, CuO, NiO and many more have been explored and widely used because of their excellent electrical, optical, catalytic and magnetic properties which are strongly dependent on their size and shape (Aravindan et al., 2013, Elumalai et al., 2013, Kumar et al., 2011, Kumar et al., 2012, Maiyalagan et al., 2013). The synthesis and fabrication of these nanomaterials

\* Corresponding author at: Tel.: (+65) 6516 2216, Fax: (+65) 67791459  
E-mail address: [mpesuja@nus.edu.sg](mailto:mpesuja@nus.edu.sg) (J. Sundaramurthy); [seeram@nus.edu.sg](mailto:seeram@nus.edu.sg) (S. Ramakrishna)

morphology, and porosity have been intensively pursued not only for fundamental scientific interest but also for many technological applications.

Many approaches such as sol-gel, hydrothermal, chemical vapor-deposition, electrochemical anodization and electrospinning have been utilized for the synthesis of nanostructured materials with different morphologies and shapes (Lakshmi et al., 1997, Liu et al., 2003, Sundaramurthy et al., 2012, Tsuchiya et al., 2005, Yang et al., 2004). Among the methods for preparing nanomaterials, electrospinning has attracted much attention because it provides a cost-effective, versatile, simple and continuous process. Electrospinning techniques use electric forces to drive the spinning process and to produce polymer, ceramic, and carbon/graphite fibers with diameters typically ranging from tens to hundreds of nanometers (commonly known as electrospun nanofibers). This approach has led to the synthesis of nanomaterials with pure phase, higher crystallinity, larger surface area to volume ratio, controlled morphologies with single and combinations of materials such as hollow and core/shell structures. The electrospun nanostructures have been widely used in biomedical, energy, coating, electrical, magnetic and electrochemical applications (Hamadiani et al., 2014, Kim et al., 2014, Ma et al., 2014, Sun et al., 2014, Xue et al., 2014). In this review, we will discuss the prospects of electrospun nanomaterials in energy and environmental related applications such as photocatalysis, dye sensitized solar cells (DSSCs), hydrogen generation and also storage.

## 2. Photocatalysis

The increasing industrial needs and growing urbanization have led to water scarcity issues around the globe and the wastewater produced has to be treated for re-utilization of clean water in daily activities. Among the various techniques, the heterogeneous photocatalysis system is an effective method for treating wastewater and photodegrading organic pollutants. The semiconductor metal oxides have been used as photocatalysts where upon irradiation of sunlight, create electron-hole pairs which in turn produce radicals in different pathways as shown in Figure 1 (Teoh et al., 2012).

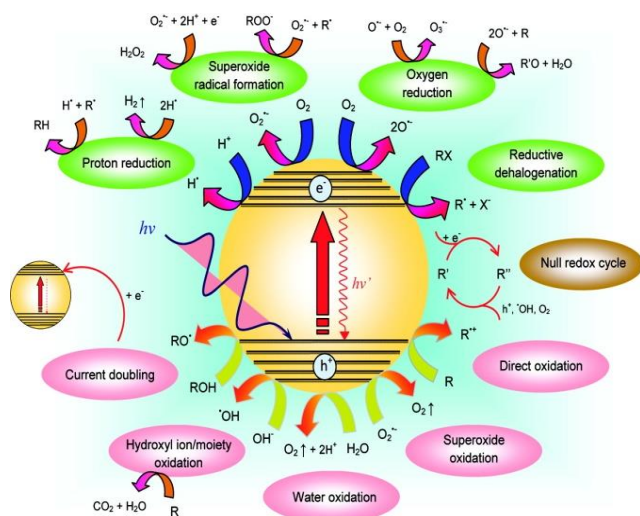


**Fig.1.** Possible photocatalytic mechanism of generating free radicals in the conduction band (CB) and valence band (VB) of semiconducting metal oxides. Reprinted with permission from Ref. (Teoh et al., 2012). Copyright (2013) American Chemical Society.

The photocatalytic mechanism is as follows: upon irradiation semiconductor metal oxides eject an electron from the valance band to the conduction band, thereby leaving behind a hole in the valence band. The generated electrons and holes produce superoxide radicals to degrade the pollutants by reacting with chemisorbed oxygen on the catalyst surface and oxygen in the aqueous solution (Bhatkhande et al., 2002, Chong et al., 2010, Han et al., 2009, Sundaramurthy et al., 2012).

Semiconducting metal-oxides such as  $\text{TiO}_2$ ,  $\text{ZnO}$ ,  $\text{Fe}_2\text{O}_3$ ,  $\text{WO}_3$ ,  $\text{Bi}_2\text{WO}_6$ ,  $\text{CuO}$  and many more have been widely used as oxidative photocatalysts for effective removal of industrial pollutants and wastewater treatment (Alves et al., 2009, Kumar et al., 2012, Lee et al., 2014, Sundaramurthy et al., 2012,

Szilágyi et al., 2013). Shengyuan et al. (2011) synthesized novel rice grain-shaped  $\text{TiO}_2$  mesostructures by electrospinning and observed the phase change with increasing temperature from  $500^\circ\text{C}$  to  $1000^\circ\text{C}$ . A comparison study was performed on the photocatalytic activity of the  $\text{TiO}_2$  rice grain and P-25. They observed an enhanced photocatalytic activity on alizarin red dye in rice grain-shaped  $\text{TiO}_2$  which was due to its single crystalline nature and larger surface area than P-25. Meng et al. (2011) synthesized anatase  $\text{TiO}_2$  nanofibers by utilizing a simple electrospinning technique and were able to grow high dense rutile  $\text{TiO}_2$  nanorods along the fibers using hydrothermal treatment. The nanofibril-like morphology of  $\text{TiO}_2$  nanorods/nanofibers with rutile and anatase phase was able to degrade the rhodamine-6G effectively under UV radiation. Zhang et al. (2012c) adopted the core/shell technique for synthesizing hollow mesoporous  $\text{TiO}_2$  nanofibers with a larger surface area of around  $118 \text{ m}^2/\text{g}$ . The hollow porous morphology of  $\text{TiO}_2$  nanofibers resulted in better interaction with rhodamine B and photodegraded it effectively in the short span of 90 min (Figure 2).

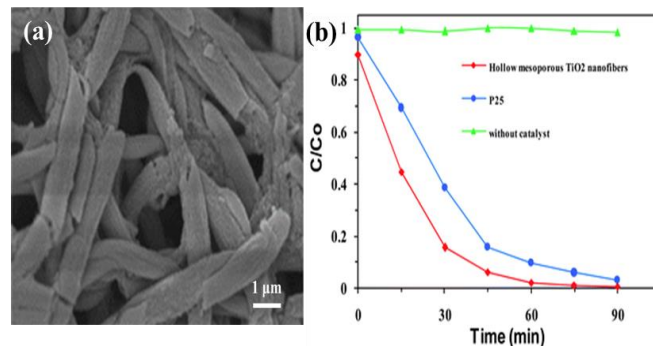


**Fig.2.** (a) FESEM image of hollow mesoporous  $\text{TiO}_2$  nanofibers and (b) photocatalytic comparison of hollow mesoporous  $\text{TiO}_2$  nanofibers and P-25  $\text{TiO}_2$  nanoparticles. Reproduced from Ref. (Zhang et al., 2012c) with permission from The Royal Society of Chemistry.

Similarly, Singh et al. (2013) was able to show the synthesis of highly mesoporous  $\text{ZnO}$  nanofibers from electrospinning with high crystallinity and large surface area. The fibers had better interaction with polycyclic aromatic hydrocarbons such as naphthalene and anthracene due to the higher surface to volume ratio of the nanofibers, and thereby had higher rate constants for the UV light photodegradation of the aromatic compounds.

Ganesh et al. (2012) demonstrated the superhydrophilic coating of  $\text{TiO}_2$  films on glass substrates using electrospinning with the film acting as a self-cleaning coating for photodegradation of alizarin red dye. The self-cleaning property of the  $\text{TiO}_2$  can be easily adopted on solid surfaces like stainless steel and also fabrics. Bedford et al. (2010) synthesized photocatalytic self-cleaning textile fibers using coaxial electrospinning where cellulose acetate was used as core fiber and  $\text{TiO}_2$  nanofiber as shell. They studied the self-cleaning photocatalytic performance of  $\text{TiO}_2$  based textile fibers by photodegradation of dyes like keyacid blue and sulforhodamine at moderate exposure of light and were able to degrade it significantly. Neubert et al. (2011) fabricated the fibrous conductive catalytic filter membrane consisting of non-conductive polyethylene oxide blended with ( $\pm$ )-camphor-10-sulfonic acid doped conductive polyaniline. They were able to incorporate the  $\text{TiO}_2$  nanoparticles on the membrane by electrospinning and achieved the photodegradation of 2-chloroethyl phenyl sulfide pollutant upon UV exposure.

However, the usage of metal oxides such as  $\text{TiO}_2$ ,  $\text{ZnO}$ ,  $\text{SnO}_2$  and  $\text{Fe}_2\text{O}_3$  for practical applications is still limited because of the fast electron-hole recombination and broad bandgaps which respond only to UV light. Therefore, it is essential to improve the visible light absorption and other shortcomings to ameliorate the photocatalytic property by either combining with graphene, other semiconducting metal oxides or metal nanoparticles with matching bandgap (Bao et al., 2011, Pant et al., 2013, Su et al., 2013, Yousef et al., 2012, Yousef et al., 2013). Peining et al. (2012) synthesized  $\text{TiO}_2$  nanofibers incorporated with graphene and compared the photocatalytic and photovoltaic performance with  $\text{TiO}_2$  and mechanically mixed  $\text{TiO}_2$  and graphene. The better percolation of graphene into the  $\text{TiO}_2$  matrix during electrospinning was attributed to the enhanced absorption in the visible and near-IR regions. Thus, the graphene loaded  $\text{TiO}_2$  nanofibers showed an enhanced photodegradation of methyl orange than the pure  $\text{TiO}_2$  and

mechanically mixed graphene and TiO<sub>2</sub> nanofibers. Zhu et al. (2013) combined the characteristics of SnO<sub>2</sub> and Fe<sub>2</sub>O<sub>3</sub> to form heterojunction SnO<sub>2</sub>/Fe<sub>2</sub>O<sub>3</sub> nanotubes to act as an effective catalyst for the photodegradation of rhodamine B (RhB) dye under visible light exposure. Due to the wide band gap of SnO<sub>2</sub> nanotubes and upon irradiation of visible light, the electron-hole pairs were not produced effectively whereas Fe<sub>2</sub>O<sub>3</sub> have the tendency to absorb visible light and create electron-hole pairs. Thus, these heterojunction nanotubes resulted in higher visible light adsorption than the SnO<sub>2</sub> nanotubes and Fe<sub>2</sub>O<sub>3</sub> nanofibers due to the efficient separation of photoinduced electron-hole pairs created by the matching energy band configurations between them (Figure 3a). They observed a higher visible light photocatalytic activity of heterojunction nanotubes compared with the SnO<sub>2</sub> nanotubes and Fe<sub>2</sub>O<sub>3</sub> nanofibers for the degradation of RhB dye upon exposure to visible light.

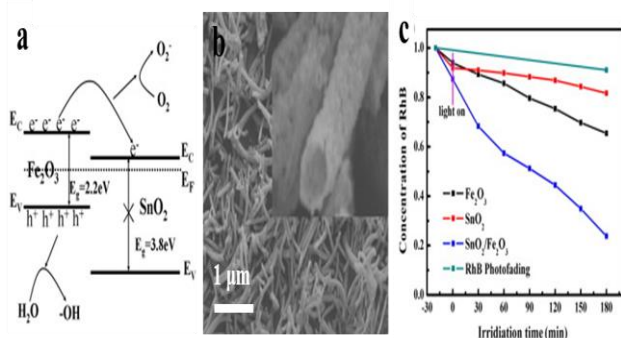


**Fig.3.** (a) Schematic of the energy band configuration of SnO<sub>2</sub>/Fe<sub>2</sub>O<sub>3</sub> heterojunctions, (b) SEM image of SnO<sub>2</sub>/Fe<sub>2</sub>O<sub>3</sub> nanotubes after calcination at 700 °C, (the inset: magnified image) and (c) concentration profile of RhB versus the visible light exposure time with photocatalysts: SnO<sub>2</sub> nanotubes, Fe<sub>2</sub>O<sub>3</sub> nanofibers, SnO<sub>2</sub>/Fe<sub>2</sub>O<sub>3</sub> nanotubes and RhB photofading irradiation. Reprinted from Ref. (Zhu et al., 2013), Copyright (2013), with permission from Elsevier.

Yuan et al. (2012) have successfully demonstrated the removal of elemental mercury (Hg<sup>0</sup>) from simulated coal combustion flue gases by utilizing the electrospun TiO<sub>2</sub> nanofibers. They observed a significant reduction in mercury when utilizing TiO<sub>2</sub> nanofibers doped with semiconducting metal oxides such as WO<sub>3</sub>, V<sub>2</sub>O<sub>5</sub>, Ag<sub>2</sub>O, In<sub>2</sub>O<sub>3</sub> and CuO. Upon combining with these metal oxides, the UV-visible light absorption intensity of metal oxides with TiO<sub>2</sub> increased significantly compared to that of pure TiO<sub>2</sub>. The absorption bandwidth also widened. They demonstrated that WO<sub>3</sub> doped TiO<sub>2</sub> fibers were able to successfully remove 100% of Hg<sup>0</sup> from flue gases under UV radiation whereas V<sub>2</sub>O<sub>5</sub> doped TiO<sub>2</sub> showed an enhanced Hg<sup>0</sup> removal efficiency from 6% to 63% under visible light irradiation. Also, doping metal oxides with non-metal elements (B, C, N, S, F) enhanced the photocatalytic activity (Di Camillo et al., 2012, Kim et al., 2012, Samadi et al., 2012). Li et al. (2012a) showed that the nitrogen doped TiO<sub>2</sub> nanofibers were able to photodegrade the RhB dye upon visible light exposure about 12 times more than the TiO<sub>2</sub> nanofibers. They nitride the TiO<sub>2</sub> fibers by treating in ammonia flow at 500 °C and the doping improved the visible light response due to the formation of the oxygen vacancies and Ti-O-N bonding.

As discussed earlier, the combination of semiconductor metal-oxides with matched band gap configuration enhances the photocatalytic activity. Similarly, the metallic nanoparticles combined with the semiconducting metal oxides possess synergetic properties and improve the photocatalysis significantly (Alves et al., 2013, Madhavan et al., 2012, Song et al., 2013). Guan et al. (2013) have observed an enhanced photodegradation of RhB using Ag nanoparticles (NPs) coated TiO<sub>2</sub> nanofibers upon exposure to sunlight. They employed silver mirror reaction to incorporate the NPs in nanofibers and observed that the loading capacity of AgNPs plays a role in photocatalysis. In Ag NP loaded TiO<sub>2</sub> nanofibers, the Ag readily absorbs the electrons in the conduction band of TiO<sub>2</sub> due to its lower work function than the lower conduction band edge of TiO<sub>2</sub> and avoids the recombination of electrons with the holes. In addition, the Schottky barrier effect prevents electrons from moving from Ag into the TiO<sub>2</sub> acting as the electron trap sites. Also, the electrons excited from the Ag are involved in plasmonic energy transfer from Ag to the dye, thus further enhancing the dye degradation.

Zhang et al. (2012a) synthesized heterojunction TiO<sub>2</sub>/ZnO nanofibers using simple electrospinning and then embedded Au nanoparticles into the fibers by using the in-situ reduction approach. They were able to demonstrate that the three ways synergistic effect of TiO<sub>2</sub>/ZnO/Au led to higher charge separation under ultraviolet excitation and thereby inducing higher photodegradation of methyl orange and 4-nitrophenol compared to pure TiO<sub>2</sub> and ZnO nanofibers. The charge transfer mechanism is similar as discussed in AgNPs incorporated in TiO<sub>2</sub> where the electrons in the conduction band of TiO<sub>2</sub> were trapped by the Au due to its high Schottky barrier and reducing the recombination. Also, the bandgap matching of ZnO and TiO<sub>2</sub> nanofibers promoted electron transferring from the conduction band of ZnO to the conduction band of TiO<sub>2</sub> whereas the electrons were irreversibly transferred on the surface of Au due to its lower work function, while the holes in the valence band of TiO<sub>2</sub> were trapped in the valence band of ZnO, leading to effective charge separation (Figure 4a). This phenomenon was further evidenced by the photoluminescence quenching of UV emission of ZnO nanofibers (Figure 4b).

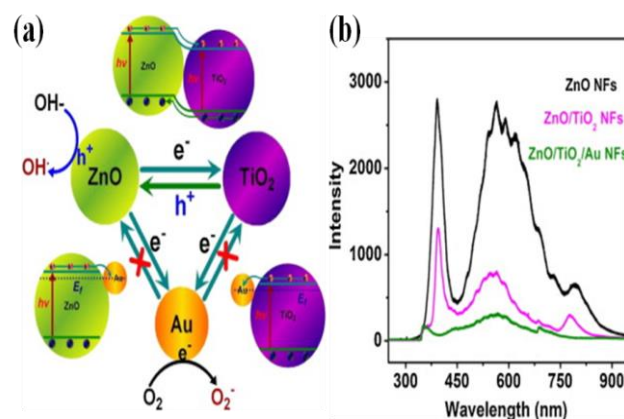


**Fig.4.** (a) The possible mechanism for three ways synergistic of TiO<sub>2</sub>/ZnO/Au system for UV light-induced photodegradation, and (b) photoluminescence emission spectra of the pure ZnO, TiO<sub>2</sub>/ZnO and TiO<sub>2</sub>/ZnO/Au nanofibers. Reprinted from Ref. (Zhang et al., 2012a), Copyright (2013), with permission from Elsevier.

The combination of metal-oxides in nanofibers can be obtained differently from the routes discussed earlier like doping or addition of metal oxides. One of the approaches is forming core/shell nanostructures of metal oxides where a metal oxide layer acts as a shell and another as core layer (Zhang et al., 2012b). Electrospinning technique is one of the very effective techniques in synthesizing core/shell nanostructures in different combinations of metal oxides. Peng et al. (2012b) fabricated highly uniform SnO<sub>2</sub>/TiO<sub>2</sub> coaxial nanoscale fibers by employing electrospinning and were able to photodegrade RhB dye effectively. They were able to tune the surface area of metal oxides by synthesizing solid and hollow core/shell nanostructures with an area of 60 m<sup>2</sup>/g and 87 m<sup>2</sup>/g, respectively, higher than the pure TiO<sub>2</sub> nanofibers and Degussa nanoparticles. The well-defined heterojunction created between SnO<sub>2</sub>/TiO<sub>2</sub> led to an increase in charge-separation and efficient interparticle charge transfer along the nanofiber. The hollow structure with high surface area allowed the full exposure of dye molecules to both layers, allowing both photogenerated electron-hole pairs to participate in the photocatalysis reaction effectively.

### 3. Dye Sensitized Solar Cells (DSSCs)

The basic working principle of DSSC is the photoexcitation of dye resulting in electron injection into the conduction band of the metal oxide (which acts as photoanode) and the hole injection into the electrolyte (Figure 5). The metal oxide anode is percolated with an electrolyte whose redox potential supports the separation of bound electron-hole pairs in the metal oxide and photoexcited dye (Thavasi et al., 2009). Electrospun metal oxides (TiO<sub>2</sub>, ZnO, SnO<sub>2</sub>, and CuO) and its composites with CNTs/graphene have been widely used for DSSCs.

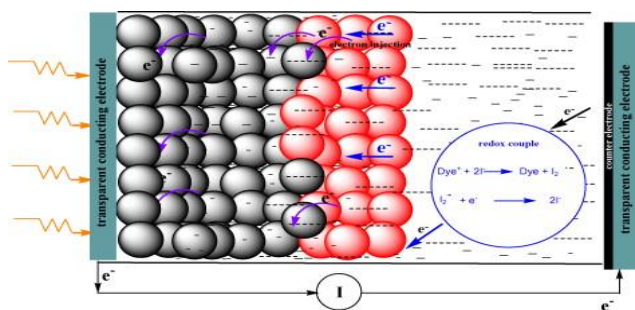


**Fig.5.** Schematic diagram of dye sensitized solar cells. Reprinted from Ref. (Thavasi et al., 2009), Copyright (2013), with permission from Elsevier.

Kumar et al. (2012) have reported highly crystalline hierarchical TiO<sub>2</sub> nanostructures ranging from one-dimensional regular fibers, hollow tubes, porous rods and spindles by changing annealing temperatures (Figure 6).

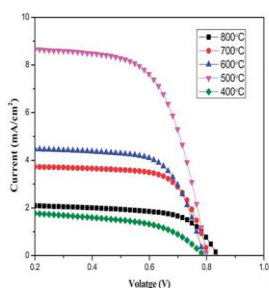


**Table 1** Device characteristics of DSSCs with different hierarchical TiO<sub>2</sub> nanostructure electrodes

Annealing temperature/°C	Hierarchical TiO <sub>2</sub> morphology	V <sub>oc</sub> /V	J <sub>sc</sub> /mA cm <sup>-2</sup>	FF (%)	η (%)
400	Spindle	0.765	1.98	52.1	0.79
500	Porous rod	0.798	8.61	66.3	4.56
600	Rod structure	0.782	4.55	69.5	2.47
700	Hollow tube	0.798	3.79	71.5	2.16
800	Spindle network	0.832	2.18	64.6	1.17

**Fig.6.** Photocurrent density-voltage characteristics of DSSCs with different hierarchical TiO<sub>2</sub> nanostructure electrodes. Reproduced from Ref. (Kumar et al., 2012) with permission from The Royal Society of Chemistry.

A higher conversion efficiency ( $\eta$ ) of 4.56% with a short circuit current ( $J_{sc}$ ) of 8.61 mA/cm<sup>2</sup> was observed for highly ordered porous anatase TiO<sub>2</sub> nanorods obtained upon annealing at 500 °C under simulated AM 1.5, confirming that the surface area of TiO<sub>2</sub> resulting from a porous structure played a dominant role (Table 1).

**Table 1**

Summary of the hydrogen storage capacity for the electrospun carbon nanofibers.

Carbon Sources	Solvent	Incorporated Compounds	Activation Agent	Testing Temperature	Testing Pressure	Hydrogen Capacity	Remarks
PAN	DMF	...	Water Vapor	77 K	1 bar	2.36 wt%	Ref (Kim et al., 2011)
		PdCl <sub>2</sub>		298 K		0.10 wt%	
				77 K		1.83 wt%	
				298 K		0.82 wt%	
PAN	DMF	V <sub>2</sub> O <sub>5</sub>	KOH	303 K	100 bar	2.5 wt%	Ref (Im et al., 2009b)
		Fluoride				3.2 wt%	
PAN	DMF	Fe <sub>2</sub> O <sub>3</sub>	KOH	RT	100 bar	1.33 wt%	
		MgO				1.69 wt%	Ref (Im et al., 2009a)
		CuO				2.77 wt%	
		Fe				2.05 wt%	
		Mg				2.29 wt%	
PAN	DMF	...	KOH	303 K	50 bar	1.03 wt%	Ref (Im et al., 2008c)
		ZnCl <sub>2</sub>				1.54 wt%	
PAN	DMF	...	NaOH	303 K	50 bar	1.05 wt%	Ref (Im et al., 2009c)
		K <sub>2</sub> CO <sub>3</sub>				0.39 wt%	
PVdF	DMF	...	...	RT	80 bar	0.39 wt%	Ref (Hong et al., 2007)
		Iron (III) acetylacetonate				0.18 wt%	
PAN	DMF	V <sub>2</sub> O <sub>5</sub>	KOH	RT	100 bar	2.41 wt%	Ref (Im et al., 2008a)
PAN	DMF	MgCl <sub>2</sub>	...	303 K	50 bar	26	Ref (Jung et al., 2009)
						mmol/cm <sup>3</sup>	
PAN	DMF	Iron (III) acetylacetonate	...	RT	100 bar	1.01wt%	Ref (Kim et al., 2005)
PANI	DI Water	...	...	298-398 K	80 bar	3-10 wt%	Ref (Srinivasan et al., 2010)
PCS	...	...	...	77 K	1 bar	2.75 wt%	Ref (Rose et al., 2010)
					17 bar	3.86 wt%	

PAN: Polyacrylonitrile;

PVdF: Poly(vinylidene fluoride)

PANI: Polyaniline

PCS: Polycarbomethylsilane

DMF: N,N dimethylformamide

RT: Room temperature

He et al. (2013) have prepared two types of electrospun TiO<sub>2</sub> nanotubes by co-axial electrospinning followed by pyrolysis of electrospun core-shell nanofibers. The structural and surface analysis confirms that both types of TiO<sub>2</sub> nanotubes possess anatase phase structure with fiber diameters of ~400-500nm. DSSC with photoanode based TiO<sub>2</sub> nanotubes have higher short-circuit current density ( $J_{sc}$  of 7.15 mA/cm<sup>2</sup>) with device efficiency around  $\eta=3.80\%$ . Jung et al. (2012) have synthesized anatase TiO<sub>2</sub> nanofibers with a thickness of 80-150 nm, specific surface area of 103.3 m<sup>2</sup>/g with porosity of 80.5% and were able to obtain an efficiency of 4.6%, which was significantly higher than that of the typical TiO<sub>2</sub> nanofibers. Nair et al. (2012) reported highly porous, dense, and anisotropic TiO<sub>2</sub> derived from electrospun TiO<sub>2</sub>-SiO<sub>2</sub> nanostructures through titanate route. The titanate-derived TiO<sub>2</sub> of high surface areas exhibited superior photovoltaic parameters ( $\eta>7\%$ ) in comparison to respective electrospun TiO<sub>2</sub> nanomaterials and commercially available P-25. Bijarbooneh et al. (2013) have reported mesoporous anatase TiO<sub>2</sub> nanofibers with a diameter of around 300 nm and 10-20  $\mu\text{m}$  length show a conversion cell efficiency of 8.14%, corresponding to a ~35% enhancement over the Degussa P25 reference photoanode.

Zhang et al. (2012b) reported hollow mesoporous TiO<sub>2</sub> nanofibers prepared by co-axial electrospinning with two immiscible polymers, polyethylene oxide (PEO) and polyvinylpyrrolidone (PVP) (Figure 7a&b).

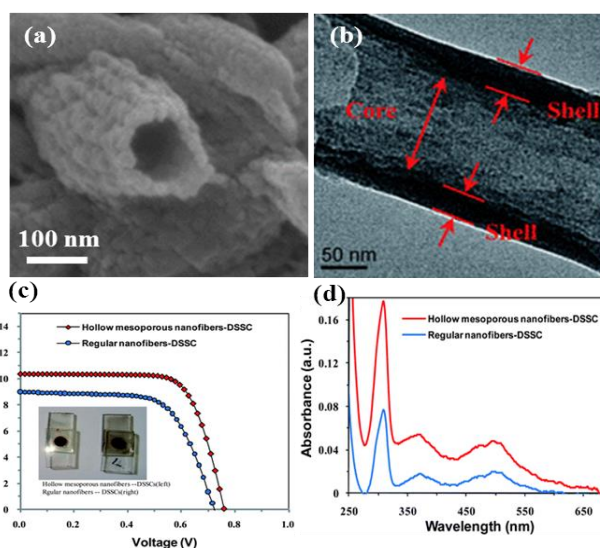


**Fig.7.** (a) FESEM image of hollow mesoporous TiO<sub>2</sub> nanofibers; (b)TEM image of core-shell (PEO/TiO<sub>2</sub>-PVP) composite nanofibers; (c) Photocurrent density-voltage curves of DSSC constructed with TiO<sub>2</sub> as photoanode using hollow mesoporous nanofibers and regular nanofibers (right) based cell; (d) UV-vis absorption spectra of the absorbed dye molecules on TiO<sub>2</sub> hollow mesoporous and TiO<sub>2</sub> regular nanofibers. Reproduced from Ref. (Zhang et al., 2012b) with permission from The Royal Society of Chemistry.

The solar-to-current conversion efficiency ( $\eta$ ) and short circuit current ( $J_{sc}$ ) of these nanofibers were measured to be around 5.6% and 10.38 mA/cm<sup>2</sup> respectively, which were higher than those of DSSC made using regular TiO<sub>2</sub> nanofibers under identical conditions ( $\eta=4.2\%$ ,  $J_{sc} = 8.99$  mA/cm<sup>2</sup>) (Figure 7c). The improved efficiency was due to the higher absorption of dye molecules on the hollow mesoporous TiO<sub>2</sub> interfacial surface area (Figure 7d). Chen et al. (2013) have fabricated ultraporous anatase TiO<sub>2</sub> nanorods with a composite structure of mesopores and macropores via a simple microemulsion electrospinning process. In this approach, a high power conversion efficiency of 6.07% was obtained for the porous TiO<sub>2</sub> nanorod based DSSCs and bilayer structured photoanode with porous TiO<sub>2</sub> nanorods acting as the light scattering layer showing an enhanced efficiency of 8.53%. Hwang et al. (2012) have reported multiscale porous TiO<sub>2</sub> nanofibers fabricated through electrospinning and etching processes with TiO<sub>2</sub>/SiO<sub>2</sub> composite nanofibers for high-efficiency DSSCs. The surface area of the mesoporous TiO<sub>2</sub> nanofibers was reported to be 9 times higher than that of pristine TiO<sub>2</sub> nanofibers, providing sufficient dye adsorption for light

harvesting as well as efficient paths for electrolyte contact. DSSCs exhibited an enhanced current density ( $J_{sc}$ ) of 16.3 mA/cm<sup>2</sup> and high photoconversion efficiency ( $\eta$ ) of 8.5%, greater than those of conventional photoelectrodes made of TiO<sub>2</sub> nanoparticles ( $J_{sc}$  of 12.0 mA/cm<sup>2</sup> and  $\eta$  of 6.0%). Song et al. (2005) demonstrated TiCl<sub>4</sub> treated electrospun TiO<sub>2</sub> electrode with rutile crystals grown epitaxially on anatase TiO<sub>2</sub> fibers able to increase the adsorption of sensitizers. The incident photon-to-current conversion efficiency (IPCE) of TiCl<sub>4</sub>-treated electrode was higher than the untreated fiber. The photocurrent of the DSSC with electrospun TiO<sub>2</sub> electrode was enhanced by more than 30% after TiCl<sub>4</sub> treatment.

Kim et al. (2009) have prepared poly (vinylidene fluoride-co-hexafluoropropylene) (PVDF-HFP) based nanofibers polymer electrolytes by the electrospinning method and adapted to the polymer matrix in polymer electrolytes for DSSCs. The uptake, ionic conductivity and porosity of the electrospun PVDF-HFP nanofiber films showed 653±50%, 4.53±1.3×10<sup>-3</sup> S/cm, and 70±2.3%. Park et al. (2011) have prepared electrospun PVDF-HFP and PVDF-HFP/polystyrene (PS) blends nanofibers electrolytes. The best results for  $V_{oc}$ ,  $J_{sc}$ , FF and efficiency of the DSSC devices using the electrospun PVDF-HFP/PS (3:1) blend nanofibers were 0.76V, 11.8mA/cm<sup>2</sup>, 0.66 and 5.75% under AM1.5. Ahn et al. (2012) have reported electrospun PVdF-co-HFP polymer gel electrolyte with and without doping with the liquid crystal E7 and with a liquid electrolyte. The ionic conductivity of E7 embedded on PVdF-co-HFP polymer gel electrolyte was found to be 2.9 × 10<sup>-3</sup> S/cm which is 37% higher than that of PVdF-co-HFP polymer gel electrolyte. The DSSCs containing the E7 embedded PVdF-co-HFP polymer gel electrolyte was observed to possess a higher power conversion efficiency (PCE = 6.82%) than that of PVdF-co-HFP nanofiber (6.35%). Park et al. (2013) have prepared hollow activated carbon nanofibers by concentric electrospinning of poly (methyl methacrylate) as a pyrolytic core precursor and polyacrylonitrile as a carbon shell precursor, followed by stabilization, carbonization, and activation. The activated nanofibers with high mesoporosity possessed a total surface area of 1037.5 m<sup>2</sup>/g with a mesoporous surface area of 97.9 m<sup>2</sup>/g, and total pore volume of 0.70 m<sup>3</sup>/g which were adopted as counter electrodes for DSSCs. Barakat et al. (2012) prepared Pd-Co-doped carbon nanofibers using low cost and effective electrospinning technique. As a counter electrode material in DSSC, nanofibers revealed good performance with relatively high short-circuit current density ( $J_{sc}$ ) of 9.8 mA/cm<sup>2</sup> and open circuit voltage ( $V_{oc}$ ) of 0.705 V. Besides the known catalytic activity, the utilized metallic carbon nanofibers revealed a band gap of 4.7 eV which simultaneously enhances iodine reduction on the electrode surface. Peng et al. (2012a) have reported electrospun conductive polyaniline doped with 10-camphorsulfonic acid (PANI-CSA) blended with polylactic acid composite nanofibers as counter electrodes. The photoelectric conversion efficiency of the DSSCs of the rigid and flexible PANI-CSA-PLA counter electrodes were 5.3% and 3.1% under AM 1.5, respectively, which was well close to the efficiencies obtained from sputtered with Pt-based counter electrode DSSCs.

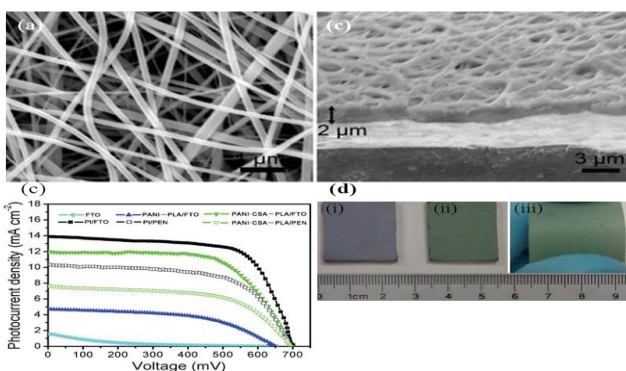


**Fig.8.** (a) SEM image and (b) cross-sectional view of the PANI-CSA-PLA nanofiber film; (c) Photocurrent density-voltage (J-V) curves of DSSCs based on FTO glass, PANI-PLA/FTO, PANI-CSA-PLA/FTO, Pt/FTO, PANI-CSA-PLA/PEN, and Pt/PEN counter electrodes respectively, under 1 sun illumination of 100 mW/cm<sup>2</sup>(AM 1.5); and (d) the photos of the (i) PANI-PLA/FTO, (ii) PANI-CSA-PLA/FTO, and (iii) PANI-CSA-PLA/PEN nanofiber films, respectively. Reproduced from Ref. (Peng et al., 2012) with permission from The Royal Society of Chemistry.

Moreover, Li et al. (2011) have prepared silver nanoparticle doped TiO<sub>2</sub> nanofibers as the photoanode through the electrospinning process to fabricate DSSCs. When compared with the undoped DSSC sample, the short circuit current density of the Ag doped DSSC sample improved by 26% resulting in a conversion efficiency improvement of 25%. Nair et al. (2011) have fabricated electrospun TiO<sub>2</sub> nanorod-based efficient photoanode using a Pechini-type sol. The Pechini-type sol of TiO<sub>2</sub> nanofibers produces a highly porous and compact layer of TiO<sub>2</sub> upon doctor-blading and sintering without the need for an adhesion and scattering layers or TiCl<sub>4</sub> treatment. The best nanofiber DSSCs within an area of 0.28 cm<sup>2</sup> shows an efficiency of ~4.2% under standard test conditions and an IPCE of ~50%. Yun et al. (2011) have synthesized electrospun Al-doped ZnO nanofiber electrodes with energy conversion efficiency ( $\eta$ ) of 0.54-0.55% under irradiation of AM1.5 simulated sunlight. Lin et al. (2012) reported electrospun 1-D mesoporous anatase TiO<sub>2</sub> nanofibers combined with a sol-gel process using 0-3 wt % of room-temperature ionic liquid as the mesopore formation template. The performance of the DSSCs fabricated with TiO<sub>2</sub> nanofibers with ionic liquids was significantly higher than that of electrospun TiO<sub>2</sub> nanofibers without ionic liquids. TiO<sub>2</sub> nanofibers with 1 wt% ionic liquid had the largest improvement (~50.4%) in energy conversion efficiency (5.64%) over that of pure TiO<sub>2</sub> nanofibers without ionic liquid (3.75%). The enhancement in the efficiency was attributed to the unique morphology of nanofibers, which led to more dye loading, faster electron transportation, and higher charge collection efficiency.

Sahay et al. (2012b) have adopted copper based composite nanofibers by using the copper acetate/polyvinyl alcohol/water solution as the starting material. The effect of the annealing cycle on the crystalline structure showed that a decrease in crystallite size with an increase in the dwelling time improved the orientation of the CuO crystallite. The results suggested a 25% increase in the current density with CuO as blocking layer in ZnO based DSSC. Zhang et al. (2009) have reported tunable thickness of wurtzite ZnO nanofiber photoelectrodes as self-relaxation layer. This layer facilitated the release of interfacial tensile stress during calcination, resulting in good adhesion of the ZnO film to FTO substrate. By controlling the electrospinning time, the film thickness has been tuned from 0 to 5 μm. The improved cell performance with increased film thickness were observed due to the improvement in short-circuit current density ( $J_{sc}$ ), which was explained by the larger surface area of the ZnO film with an increased thickness and thus higher dye loading. Similarly, Kim et al. (2007b) have reported electrospun ZnO/ poly (vinyl acetate) composite nanofiber mats coated with FTO and calcined at 450 °C. The multiple nanofiber networks composed of a twisted structure with a diameter of around 200-500 nm cores and grains size with 30 nm. The DSSCs using ZnO nanofiber mats exhibited a conversion efficiency of 1.34% under 100 mW/cm<sup>2</sup> (AM-1.5 G) illuminations. Elumalai et al. (2012) have reported an electrospun highly crystalline SnO<sub>2</sub> flower which showed lower density of surface trap states than fibers by combining absorption spectra and open circuit voltage decay measurements. The flowers showed an enhanced Fermi energy on account of which as well as higher electron mobility, DSSCs fabricated using the SnO<sub>2</sub> flowers gave  $V_{oc}$ ~700 mV and one of the highest photoelectric conversion efficiencies achieved using pure SnO<sub>2</sub>.

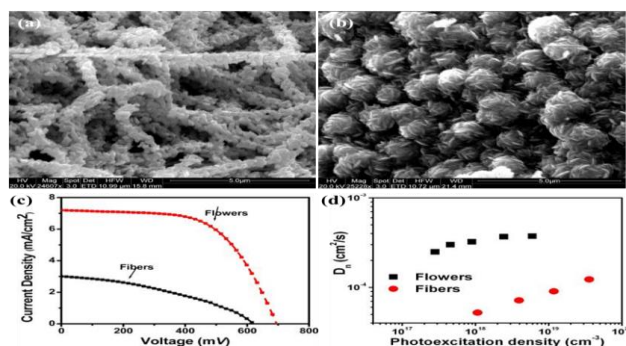


**Fig.9.** FESEM image of the (a) fibers and (b) flowers; (c) J-V characteristics of the DSSCs fabricated using flowers and fibers; and (d) Electron diffusion coefficients of the flower and fiber based devices. Reproduced from Ref. (Elumalai et al., 2012) with permission from The Royal Society of Chemistry.

Gao et al. (2012) have reported a simple procedure for using the porous SnO<sub>2</sub> nanotube-TiO<sub>2</sub> (SnO<sub>2</sub>/TiO<sub>2</sub>) core-shell structured photoanodes for DSSCs. The power conversion efficiency values of the SnO<sub>2</sub>/TiO<sub>2</sub> core-shell structured DSSCs (~5.11%) were five times higher than that of SnO<sub>2</sub> nanotube DSSCs (~0.99%). Song et al. (2013a) have prepared TiO<sub>2</sub> nanoparticles/nanofibers bilayer film via spin coating and electrospinning. The TiO<sub>2</sub> bilayer film with a thickness of about 6.0 μm was composed of anatase TiO<sub>2</sub> phase. DSSCs were assembled by hydrochloric acid treated TiO<sub>2</sub> film. The maximum photo-to-electron conversion and overall conversion efficiency (η) were obtained from 0.05 M HCl treated TiO<sub>2</sub> based DSSC about 48.0% and 4.75%, which were respectively increased by 14% and 6.3% than those of DSSC based on untreated TiO<sub>2</sub> films. Park et al. (2012) have prepared mesoporous multi-walled carbon nanotube-embedded carbon nanofibers through various steps of the electrospinning process. These mesoporous structures showed a surface area of 562 m<sup>2</sup>/g with average pore diameter of 27.32 nm and total pore volume of 1.16 cm<sup>3</sup>/g. Overall the conversion efficiency of these nanofibers increased to 6.35% which was higher than Pt counter electrode because its characteristics promoted the electron and ion transfer, decreasing the resistance of charge transfer, and increasing the contact area between liquid electrolyte and nanofibers. Anish Madhavan et al. (2012) have reported electrospun TiO<sub>2</sub>-graphene composite nanofibers as conductive nanofiber mats using polyvinylpyrrolidone. Conductivity measurements showed the mean specific conductance values obtained for TiO<sub>2</sub>-graphene composites were about two times higher than that of the electrospun TiO<sub>2</sub> fibers. TiO<sub>2</sub>-graphene composite fibers assembled as photoanodes showed an efficiency of 7.6%. Similarly, Peining et al. (2012) fabricated one-dimensional electrospun TiO<sub>2</sub>-graphene nanocomposite which showed a significant enhancement in the photovoltaic in comparison to TiO<sub>2</sub> as demonstrated in the dye-sensitized solar cells. Seo et al. (2011) investigated the effects of a brominated poly (phenylene oxide) electrospun nanofiber mat as a non-fluorinated polymer backbone in DSSCs quasi-solid-state electrolyte. The open circuit voltage increased by 50 mV and the efficiency was comparable to a conventional liquid electrolyte. Quasi-solid-state DSSCs exhibited enhanced long-term stability, maintaining about 97% of the initial efficiency after 7 d under a mild acceleration condition at 50 °C.

#### 4. Hydrogen Generation

Hydrogen is an excellent fuel gas due to its high energy density, environmental cleanness and zero carbon footprints. Back in 1972, Honda and Fujishima discovered a method to produce hydrogen through photocatalytic water-splitting using TiO<sub>2</sub> as the electrode (Honda et al., 1972). Since then, intensive efforts have been focused on the fabrication of highly efficient nanostructured electrodes for photocatalytic/photoelectrochemical hydrogen generation. Among various synthesis techniques, electrospinning has drawn much of the scientific attention because of its versatility, simplicity, and cost-effectiveness. In this section, the application of electrospun nanofibers in photocatalytic/photoelectrochemical hydrogen generation is presented. In general, the hydrogen generation process involves three steps, namely charge generation, charge separation and redox reactions. Upon light irradiation, electrons and holes are generated from the semiconducting electrode, as similar in photovoltaic solar cells. These charge carriers are then separated to avoid reverse recombination while taking part in water oxidation and reduction reactions, respectively (Figure 10). Electrospinning as a method for nanostructure fabrication is able to effectively influence all these three steps.

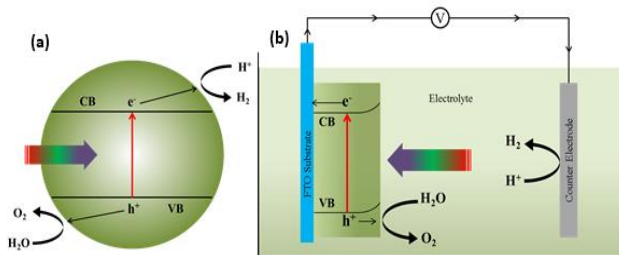


Fig.10. Schematic working mechanism of (a) photocatalytic and (b) photoelectrochemical (PEC) hydrogen generation.

It is a well-known physical phenomenon that light absorption by a semiconducting material is highly determined not only by its own physical and chemical properties, such as the band gaps, but also by its structural configurations. The limitation of pure semiconducting materials can be easily addressed by chemical modification of the electrodes like doping, which can be effectively carried out in electrospinning by simple addition of dopant salts in the electrospinning precursor solution. The introduced dopants are able to form extra energy levels within the forbidden bands, thereby reducing the energy required for valence electrons excitation up into a higher energy level. Through such mechanisms, a larger proportion of the solar spectrum can be utilized to achieve higher energy conversion efficiency. N-doped TiO<sub>2</sub> grain-like nanostructures have been successfully synthesized via electrospinning. The doped-nitrogen reduced TiO<sub>2</sub> band gap down to 2.83 eV, and increased H<sub>2</sub> generation rate up to 28 μmol/h, which was 12 times more than pristine TiO<sub>2</sub>. This superiority was mainly ascribed from the reduced band gap combined with a larger surface area (Babu et al., 2012). Compared with its nanoparticle counterparts, nanofibers demonstrate much better mesoporosity, enlarged surface area, tunable fiber morphology and aspect ratios which can significantly enhance the light scattering effect (Choi et al., 2010). Chen et al. (2012) have reported that the preferred scattering wavelength and intensity was linearly proportional to the fiber diameter and the fiber deposition density. An overlapping between scattering bands and absorption bands was much favorable for an improved photocatalytic activity since the scattered light would have a longer pathway within the material and much enhanced light absorption.

The photogenerated charge carriers have to be separated before recombination occurs. Efficient charge separation can be achieved by inducing some secondary structures within the electrospun nanofibers, or by introducing electron reservoirs or highly conducting materials on the nanofiber surface. Regarding the former approach, Chuangchote et al. (2009) had prepared 1-D nanofibrils along the electrospun TiO<sub>2</sub> nanofibers and these nanofibrils were believed to be beneficial for a higher material crystallinity as well as a retarded electron-hole recombination compared with their nanoparticle counterpart. In addition, nanofibers consisting of interconnected 0-D nanoparticles can also be achieved by directly electrospinning the nanoparticle dispersed solution (Choi et al., 2010). Within the nanofibers, TiO<sub>2</sub> nanoparticles were densely packed and closely interconnected, therefore the photogenerated charge carriers were efficiently transported away to different sites for water oxidation and reduction reactions (Figure 11).

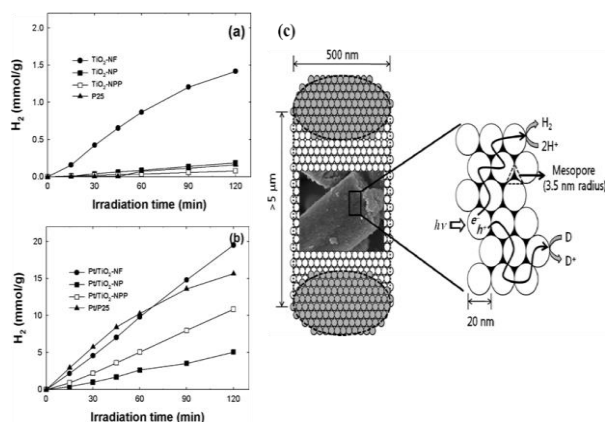


Fig.11. Time-profiled H<sub>2</sub> evolution in UV-irradiated suspensions of (a) TiO<sub>2</sub> and (b) Pt deposited TiO<sub>2</sub> (Pt/TiO<sub>2</sub>); (c) schematic illustration of the nanoparticulated nanofibers with the mechanism of charge separation and transportation. Reprinted with permission from Ref.(Choi et al., 2010). Copyright (2010) American Chemical Society.

The nanofiber structures comprised with nanoparticles can be further sensitized by Eosin-Y, and used for dye-sensitized hydrogen production (Choi et al., 2012). Upon light irradiation, Eosin-Y was excited to produce oxidized sensitizer and electrons. The electrons were then readily transferred away by the interconnected nanoparticles, while the oxidized sensitizers were reduced by the dye molecule itself.

Additionally, the nanomaterial heterojunctions with non-aligned band configuration were much more favorable for efficient charge separation due to the presence of built-in band bending, as discussed in the "Photocatalysis" section. Electrospun nanofibers with heterojunction of anatase TiO<sub>2</sub>/rutile TiO<sub>2</sub>/rutile SnO<sub>2</sub> had been successfully synthesized by Lee et al. (2012). Charge carriers were generated in all of the three metal oxides due to the similarity of their band gap width. However, because of the non-aligned energy bands, the electrons were transported to SnO<sub>2</sub> due to its lowest conduction band edge, while holes to rutile TiO<sub>2</sub> due to its highest valence band edge among the three materials. Thus, the charge carriers were efficiently separated and the recombination process was lowered to a minimum level. Another similar heterojunctional configuration was achieved by the same group (Bai et al., 2012), but in a component assembly level. A "Forest-like" photocatalyst was successfully synthesized using the electrospun anatase TiO<sub>2</sub> as the stems (200-400 nm), hydrothermally grown ZnO nanorods as twigs (100-300nm) and photo-deposited CuO nanoparticles (10-100nm) as individual leaves. These nature mimicked structures were favorable due to their hierarchical structures leading to better light absorption, and also enhanced charge separation at the various metal oxide interfaces. Highly conductive materials or electron reservoirs were also commonly used to enhance the charge separation process. Other than the commonly used Pt deposition, Yousef et al. (2012b) had managed to synthesize graphite protected Ni-doped TiO<sub>2</sub> nanofibers by sintering the nickel acetate tetrahydrate-titanium isopropoxide-PVP electrospun fiber mesh in a hydrogen/argon condition. This architecture led to superior performance not only because of the graphite protection of the catalysts, but also due to the efficient charge transportation induced by the graphite layers.

In the following hydrogen generation process, the photogenerated electrons and holes are consumed in water reduction and oxidation reactions, respectively. Therefore, the number of reactive sites as well as the activity of each individual site plays an important role in determining the H<sub>2</sub> evolution rate. By employing electrospinning, the nanomaterials with higher surface area can be easily achieved which in turn enhance the redox reactions occurring at catalyst interfaces. The electrospun nanofibers can also act as structural support for photocatalysts to increase their chemical stability while retaining the interfacial surface area. The fluoropolymer with the stable C-F bond demonstrated an excellent stability in various conditions, i.e. thermal, radiational and chemical treatment. Nanoparticles such as ZnIn<sub>2</sub>S<sub>4</sub> (Fan et al., 2010) and ZnS-AgIn<sub>5</sub>S<sub>8</sub> were successfully grown on electrospun fluoropolymer nanofibers and these materials achieved much enhanced H<sub>2</sub> evolution rate compared with nanoparticles without support (He et al., 2012). Additionally, this electrospun fluoropolymer support was used for hydride hydrolysis to produce hydrogen gas (Chinnappan et al., 2011, Chinnappan et al., 2012, Li et al., 2012). A similar concept was also applied to glucose hydrolysis using electrospun silica fiber as support and iron as catalyst (Hansen et al., 2011).

## 5. Hydrogen Storage

Storage challenges need to be addressed before using hydrogen gas as alternatives for fossil fuels, because of its volatility and combustibility in nature. Currently, three approaches have been adopted for hydrogen storage, namely cryogenic storage, high pressure vessels and storage in solid matrix. However, the cryogenic method requires a very low temperature, which significantly reduces its economic competitiveness; and high pressure vessels lead to lots of controversy on safety issues. Hence, storage in solid matrix is believed to be the most promising way for tackling the challenges in hydrogen storage (Reardon et al., 2012). In this section, the current status of the electrospun nanofibers in utilization for hydrogen storage is to be discussed in detail.

Van der Waals force of interaction plays a dominant role in hydrogen adsorption in solid matrix; therefore a larger specific surface area and total pore volume are very essential (Kim et al., 2011). Among all the possible materials, carbon draws much attention due to its larger surface area, chemical inertness, ease of synthesis, highly porous morphology and light weight (Dillon et al., 1997, Liu et al., 1999). Carbon matrix can be fabricated by different approaches, but electrospun carbon nanofibers (CNFs) have predominant advantages, such as a simple and straightforward synthetic approach by employing organic polymers dissolved in solvent as a source of carbon. Polymers such as polyacrylonitrile (PAN), poly (vinylidene fluoride) (PVdF) and many more have been utilized as the sources and solvent such as

N, N-dimethyl formamide (DMF) has been utilized due to its 426 K boiling point and excellent electrical conductivity (Im et al., 2009b). The as-electrospun fibers are then stabilized via heat treatment upon a few hundred degrees Celsius to avoid fiber softening or breaking up. Afterwards, the fiber structure needs to be carbonized to convert organic polymer into carbon at 1000°C in inert atmosphere like nitrogen. Then, the carbonized fibers are further activated to increase their specific surface area and total pore volume. The activation treatment requires a high temperature of over 1000°C with activation agents such as KOH, Na<sub>2</sub>CO<sub>3</sub>, NaOH, K<sub>2</sub>CO<sub>3</sub>, H<sub>3</sub>PO<sub>4</sub>, ZnCl<sub>2</sub>, SiO<sub>2</sub> or water vapors (Kim et al., 2011) (Im et al., 2009a, Jiang et al., 2002, Kim et al., 2007, Mitani et al., 2005). The activation mechanism differs from one activation agent to another. For example, ZnCl<sub>2</sub> was normally pre-dissolved in the electrospinning solution, and the pores were created by the escaping of Zn and Cl species; whereas in KOH activation, it was based on CO<sub>2</sub> or CO being burnt off from the fiber surface, leaving behind pores with various sizes in the fiber structure (Im et al., 2008c). The activation temperature and agent concentration play an important role in determining the resultant material morphologies (Im et al., 2009c). From the literatures, it has been confirmed that hydrogen adsorption for carbon materials at 77K is directly proportional to the specific surface area; but at room temperature, the Van der Waals physisorption could be easily overcome by hydrogen thermal motion (Hong et al., 2007), hence hydrogen capacity would be much reduced. Furthermore, both the mesopores and micropores are not actually contributing to the hydrogen storage capacity, and it is the ~0.7 nm pore that dominates the hydrogen adsorption capability (Bogdanovic et al., 1997). In such small pores, the potential filled from opposite surfaces will overlap and enhance each other, so that the acting force on hydrogen molecules (diameter of 0.41nm) are much stronger than that from micro-or mesopores (Figure 12) (Im et al., 2008b).

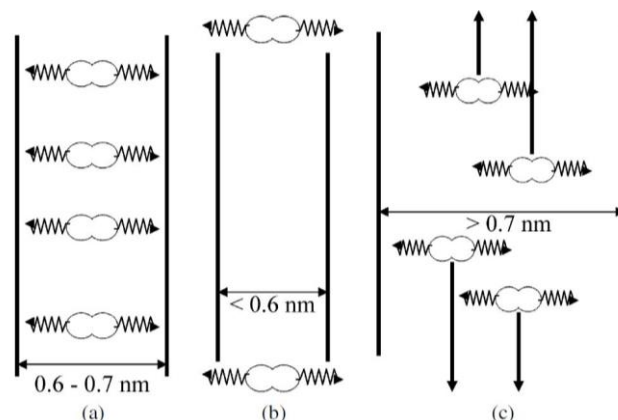


**Fig.12.** The hydrogen adsorption mechanism of pores with width of, (a) 0.6-0.7nm; (b) <0.6nm; (c) >0.7nm. Reprinted from Ref. (Im et al., 2008b), Copyright (2008), with permission from Elsevier.

It is also worth mentioning that the total volumes of such small pores are difficult to be determined by the widely used N<sub>2</sub> adsorption-desorption isotherm approach (Hong et al., 2007).

To further increase the hydrogen storage capacity, some metals or metal oxides can be incorporated into the CNFs simultaneously along with the electrospinning process, or via post treatment. The reported metals or metal oxides include MgO, Fe<sub>3</sub>O<sub>4</sub>, Mg, Fe and CuO, V<sub>2</sub>O<sub>5</sub> and MgO (Im et al., 2008a, Im et al., 2009a, Jung et al., 2009). For the metal oxides, dissociated oxygen during carbonization will generate pathways between the metal catalyst and the pore structures; therefore the hydrogen can have access to the metal catalyst embedded deep inside the fibers (Im et al., 2008a) (Figure 13).

In addition, introducing different elements with a large electronegativity gap is beneficial for hydrogen storage. For example, fluoride (F) has an electronegativity of 4.0, while that of vanadium (V) is merely 1.63. By simultaneously incorporating them into PAN-based CNFs, the hydrogen electrons can be effectively attracted to one side. Through such a mechanism, the storage capacity increased from 2.5 wt.% (for vanadium CNFs) to 3.2 wt.% (for vanadium/fluoride CNFs) at 303K and 100 bar (Im et al., 2009b).

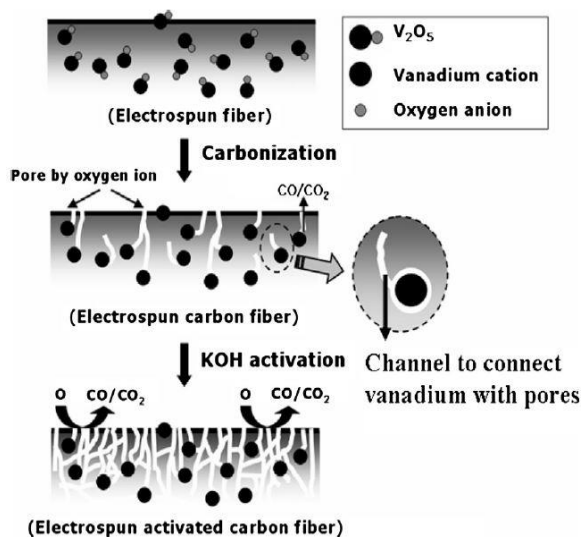


**Fig.13.** Schematic diagram of the pore formation in the  $V_2O_5$  embedded electrospun carbon fibers Reprinted from Ref. (Im et al., 2008a), Copyright (2008), with permission from Elsevier.

Other forms of carbon material, graphite for example, have also been reported to be obtainable through the electrospinning technique. Iron (III) acetylacetonate can act as catalyst for the graphitization process of the polymer fibers. The obtained graphite nanofibers (GNFs) demonstrated much larger surface areas compared to the CNFs, but no direct relation was observed between the hydrogen storage capacity and crystallinity (Hong et al., 2007, Kim et al., 2005). Highly porous carbide-derived carbon nanofibers were synthesized via electrospinning the polycarbomethylsilane (PCS) precursor followed by the pyrolysis and chlorination treatment. An extremely large surface area of  $3116 \text{ m}^2/\text{g}$  was achieved and a hydrogen storage as high as 3.86wt % at 17 bar and 77 K was reported. The hydrogen capacity at low pressure was even more impressive, reaching 2.75wt% at 1 bar and 77K, much higher than that for the bulk carbide-derived carbon materials, 2.2wt% (Rose et al., 2010). Besides the carbon materials, some other candidates were of intensive investigation for hydrogen storage application as well. Shahgaldi et al. (2012) have synthesized electrospun boron nitride nanofibers successfully. A layer of the  $TiO_2$  solution was coated by using the co-electrospinning scheme, followed by boric oxide spraying. Since B and N are both next to C in the periodic table, boron nitride depicts many similarities to carbon material, and this includes the physical and chemical properties, as well as the crystal structure. The hydrogen storage capacity for  $TiO_2$ -coated boron nitride nanofibers (BNNFs) treated at  $1300^\circ\text{C}$  demonstrated a hydrogen storage capacity of 2.1wt% at 70 bars and room temperature. Higher temperature treatment (about  $1500^\circ\text{C}$ ) reduced the capacity to 1.9wt% in identical testing conditions.

For the carbon materials in Table 1, post heating over  $1000^\circ\text{C}$  was generally required to either carbonize the polymers or to activate the electrospun nanofibers. However, Srinivasan et al. (2010) reported that electrospun PANI nanofibers can be used for hydrogen storage merely after a low temperature treatment of  $125^\circ\text{C}$  for 3 h. A reversible hydrogen storage capacity of 3-10% was observed at a temperature range of 298-398K at 80 bar. The fiber nature showed a significant morphological change before and after hydrogen adsorption, such as fiber swelling and breaking, which was seldom observed in the carbon materials. In addition, efforts were made to study metal oxide materials and their application for hydrogen storage. Electrospun ZnO nanofibers gave rise to a hydrogen capacity of 1.4wt%. Mg and Al doping increased the value to 2.29wt% and 2.81wt%, respectively, at 70 bar and room temperature (Yaakob et al., 2012). Another innovative mechanism for hydrogen storage is to encapsulate the metal or complex hydrides, such as ammonia borane into a polymer shell using co-electrospinning technique. Ammonia borane contains 19.6wt% of hydrogen,

with two thirds decomposed to gas form at  $150^\circ\text{C}$ . Encapsulating ammonia borane in a nanoporous material was able to significantly reduce the hydrogen releasing temperature down to  $85^\circ\text{C}$  and also inhibited the by-product generation (Kurban et al., 2010).

## 6. Conclusion

By employing electrospinning techniques, semiconducting metal oxide/polymer composite nanostructures with higher purity, crystallinity and aspect ratio were able to be synthesized with novel electrical, optical and catalytic properties. We have discussed here a few highlights of the application and future prospects of electrospun metal oxide nanostructures in photocatalysis, DSSCs, hydrogen generation and storage. Further, there is still a lot of potential in electrospun nanostructures in combination with other metals and metal oxides that needs to be explored. Overall, the simplicity, cost-effectiveness and ease of synthesizing metal oxide nanostructures make electrospinning an ideal candidate for materials fabrication in energy and environmental applications.

## Reference

- Ahn, S.K., Ban, T., Sakthivel, P., Lee, J.W., Gal, Y.S., Lee, J.K., Kim, M.R. and Jin, S.H., 2012. Development of dye-sensitized solar cells composed of liquid crystal embedded, electrospun poly (vinylidene fluoride-co-hexafluoropropylene) nanofibers as polymer gel electrolytes. *ACS Appl. Mater. Inter.* 4, 2096-2100.
- Alves, A.K., Berutti, F.A. and Bergmann, C.P., 2013. Visible and UV photocatalytic characterization of Sn- $TiO_2$  electrospun fibers. *Catal. Today* 208, 7-10.
- Alves, A.K., Berutti, F.A., Clemens, F.J., Graule, T. and Bergmann, C.P., 2009. Photocatalytic activity of titania fibers obtained by electrospinning. *Mater. Res. Bull.* 44, 312-317.
- Anish Madhavan, A., Kalluri, S., K Chacko, D., Arun, T.A., Nagarajan, S., Subramanian, K.R.V., Sreekumar Nair, A., Nair, S.V. and Balakrishnan, A., 2012. Electrical and optical properties of electrospun  $TiO_2$ -graphene composite nanofibers and its application as DSSC photo-anodes. *RSC Adv.* 2, 13032-13037.
- Aravindan, V., Suresh Kumar, P., Sundaramurthy, J., Ling, W.C., Ramakrishna, S. and Madhavi, S., 2013. Electrospun NiO nanofibers as high performance anode material for Li-ion batteries. *J. Power Sources* 227, 284-290.
- Arico, A.S., Bruce, P., Scrosati, B., Tarascon, J.-M. and van Schalkwijk, W., 2005. Nanostructured materials for advanced energy conversion and storage devices. *Nat. Mater.* 4, 366-377.
- Babu, V.J., Kumar, M.K., Nair, A.S., Kheng, T.L., Allakhverdiev, S.I. and Ramakrishna, S., 2012. Visible light photocatalytic water splitting for hydrogen production from N- $TiO_2$  rice grain shaped electrospun nanostructures. *Int. J. Hydro. Energy* 37, 8897.
- Bai, H., Liu, Z. and Sun, D.D., 2012. The design of a hierarchical photocatalyst inspired by natural forest and its usage on hydrogen generation. *Int. J. Hydro. Energy* 37, 13998-14008.
- Bao, N., Li, Y., Wei, Z., Yin, G. and Niu, J., 2011. Adsorption of dyes on hierarchical mesoporous  $tio_2$  fibers and its enhanced photocatalytic properties. *J. Phys. Chem. C* 115, 5708-5719.
- Barakat, N.A.M., Shaheer Akhtar, M., Yousef, A., El-Newehy, M. and Kim, H.Y., 2012. Pd-Co-doped carbon nanofibers with photoactivity as effective counter electrodes for DSSCs. *Chem. Eng. J.* 211-212, 9-15.
- Bedford, N.M. and Steckl, A.J., 2010. Photocatalytic self-cleaning textile fibers by coaxial electrospinning. *ACS Appl. Mater. Inter.* 2, 2448-2455.
- Bhatkhande, D.S., Pangarkar, V.G. and Beenackers, A.A.C.M., 2002. Photocatalytic degradation for environmental applications – a review. *J. Chem. Technol. Biotechnol.* 77, 102-116.
- Bijarbooneh, F.H., Zhao, Y., Sun, Z., Heo, Y.-U., Malgras, V., Kim, J.H. and Dou, S.X., 2013. Structurally stabilized mesoporous  $TiO_2$  nanofibres for efficient dye-sensitized solar cells. *APL Materials* 1, 032106.
- Bogdanovic, B. and Schwickardi, M., 1997. Ti-doped alkali metal aluminium hydrides as potential novel reversible hydrogen storage materials. *J. Alloys Compd.* 253-254, 1-9.
- Chen, H.Y., Zhang, T.L., Fan, J., Kuang, D.B. and Su, C.Y., 2013. Electrospun hierarchical  $TiO_2$  nanorods with high porosity for efficient dye-sensitized solar cells. *ACS Appl. Mater. Inter.* 5, 9205-9211.



- Chen, Y.-L., Chang, Y.-H., Huang, J.-L., Chen, I. and Kuo, C., 2012. Light scattering and enhanced photoactivities of electrospun Titania Nanofibers. *J. Phys. Chem. C* 116, 3857.
- Chinnappan, A., Kang, H.-C. and Kim, H., 2011. Preparation of PVDF nanofiber composites for hydrogen generation from sodium borohydride. *Energy* 36, 755-759.
- Chinnappan, A. and Kim, H., 2012. Nanocatalyst: Electrospun nanofibers of PVDF-Dicationic tetrachloronickelate (II) anion and their effect on hydrogen generation from the hydrolysis of sodium borohydride. *Inter. J. Hydro. Energy* 37, 18851.
- Choi, S.K., Kim, S., Lim, S.K. and Park, H., 2010. Photocatalytic comparison of TiO<sub>2</sub> nanoparticles and electrospun TiO<sub>2</sub> nanofibers: Effects of mesoporosity and interparticle charge transfer. *J. Phys. Chem. C* 114, 16475-16480.
- Choi, S.K., Kim, S., Ryu, J., Lim, S.K. and Park, H., 2012. Titania nanofibers as a photo-antenna for dye-sensitized solar hydrogen. *Photochem. Photobiol. Sci.* 11, 1437.
- Chong, M.N., Jin, B., Chow, C.W.K. and Saint, C., 2010. Recent developments in photocatalytic water treatment technology: A review. *Water Res.* 44, 2997-3027.
- Chuangchote, S., Jitputti, J., Sagawa, T. and Yoshikawa, S., 2009. Photocatalytic activity for hydrogen evolution of electrospun TiO<sub>2</sub> nanofibers. *ACS Appl. Mater. Inter.* 5, 1140.
- Di Camillo, D., Ruggieri, F., Santucci, S. and Lozzi, L., 2012. N-Doped TiO<sub>2</sub> nanofibers deposited by electrospinning. *J. Phys. Chem. C* 116, 18427-18431.
- Dillon, A.C., Jones, K.M., Bekkedahl, T.A., Kiang, C.H., Bethune, D.S. and Heben, M.J., 1997. Storage of hydrogen in single-walled carbon nanotubes. *Nature* 386, 377-379.
- Elumalai, N.K., Jin, T.M., Chellappan, V., Jose, R., Palaniswamy, S.K., Jayaraman, S., Raut, H.K. and Ramakrishna, S., 2013. Electrospun ZnO nanowire plantations in the electron transport layer for high-efficiency inverted organic solar Cells. *ACS Appl. Mater. Inter.* 5, 9396-9404.
- Elumalai, N.K., Jose, R., Archana, P.S., Chellappan, V. and Ramakrishna, S., 2012. Charge transport through electrospun SnO<sub>2</sub> nanoflowers and nanofibers: role of surface trap density on electron transport dynamics. *J. Phys. Chem. C* 116, 22112-22120.
- Fan, W.-J., Zhou, Z.-F., Xu, W.-B., Shi, Z.-F., Ren, F.-M., Ma, H.-H. and Huang, S.-W., 2010. Preparation of ZnIn<sub>2</sub>S<sub>4</sub>/Fluoropolymer fiber composites and its photocatalytic H<sub>2</sub> evolution from splitting of water using Xe lamp irradiation. *Int. J. Hydro. Energy* 35, 6525-6530.
- Fujishima, A., Zhang, X. and Tryk, D.A., 2007. Heterogeneous photocatalysis: From water photolysis to applications in environmental cleanup. *Int. J. Hydro. Energy* 32, 2664-2672.
- Ganesh, V.A., Nair, A.S., Raut, H.K., Walsh, T.M. and Ramakrishna, S., 2012. Photocatalytic superhydrophilic TiO<sub>2</sub> coating on glass by electrospinning. *RSC Adv.* 2, 2067.
- Gao, C., Li, X., Lu, B., Chen, L., Wang, Y., Teng, F., Wang, J., Zhang, Z., Pan, X. and Xie, E., 2012. A facile method to prepare SnO<sub>2</sub> nanotubes for use in efficient SnO<sub>2</sub>-TiO<sub>2</sub> core-shell dye-sensitized solar cells. *Nanoscale* 4, 3475-3481.
- Guan, H., Wang, X., Guo, Y., Shao, C., Zhang, X., Liu, Y. and Louh, R.-F., 2013. Controlled synthesis of Ag-coated TiO<sub>2</sub> nanofibers and their enhanced effect in photocatalytic applications. *Appl. Surf. Sci.* 280, 720-725.
- Guo, K.W., 2012. Green nanotechnology of trends in future energy: a review. *Int. J. Energ. Res.* 36, 1-17.
- Hamadani, M. and Jabbari, V., 2014. Improved conversion efficiency in dye-sensitized solar cells based on electrospun TiCl<sub>4</sub>-treated TiO<sub>2</sub> nanorod electrodes. *Int. J. Green Energy* 11, 364-375.
- Han, F., Kambala, V.S.R., Srinivasan, M., Rajarathnam, D. and Naidu, R., 2009. Tailored titanium dioxide photocatalysts for the degradation of organic dyes in wastewater treatment: A review. *Appl. Catal.*, A359, 25-40.
- Hansen, N.S., Ferguson, T.E., Panels, J.E., Park, A.-H.A. and Joo, Y.L., 2011. Inorganic nanofibers with tailored placement of nanocatalysts for hydrogen production via alkaline hydrolysis of glucose. *Nanotechnology* 22, 325302.
- He, G., Wang, X., Xi, M., Zheng, F., Zhu, Z. and Fong, H., 2013. Fabrication and evaluation of dye-sensitized solar cells with photoanodes based on electrospun TiO<sub>2</sub> nanotubes. *Mater. Lett.* 106, 115-118.
- He, M., Fan, W., Ma, H., Zhou, Z. and Xu, W., 2012. Preparation of ZnS-AgIn<sub>2</sub>S<sub>4</sub>/fluoropolymer fiber composites and its photocatalytic H<sub>2</sub> evolution from splitting of water under similar sunlight irradiation. *Catal. Commun.* 22, 89-93.
- Honda, K. and Fujishima, A., 1972. Electrochemical Photolysis of Water at a Semiconductor Electrode. *Nature* 238, 37.
- Hong, S.E., Kim, D.-K., Jo, S.M., Kim, K.Y., Chin, B.D. and Lee, D.W., 2007. Graphite nanofibers prepared from catalytic graphitization of electrospun poly(vinylidene fluoride) nanofibers and their hydrogen storage capacity. *Catal. Today* 120, 413-419.
- Hwang, S.H., Kim, C., Song, H., Son, S. and Jang, J., 2012. Designed architecture of multiscale porous TiO<sub>2</sub> nanofibers for dye-sensitized solar cells photoanode. *ACS Appl. Mater. Inter.* 4, 5287-5292.
- Im, J.S., Kwon, O., Kim, Y.H., Park, S.-J. and Lee, Y.-S., 2008a. The effect of embedded vanadium catalyst on activated electrospun CFs for hydrogen storage. *Microporous Mesoporous Mater.* 115, 514-521.
- Im, J.S., Park, S.-J., Kim, T. and Lee, Y.-S., 2009a. Hydrogen storage evaluation based on investigations of the catalytic properties of metal/metal oxides in electrospun carbon fibers. *Int. J. Hydro. Energy* 34, 3382-3388.
- Im, J.S., Park, S.-J., Kim, T.J., Kim, Y.H. and Lee, Y.-S., 2008b. The study of controlling pore size on electrospun carbon nanofibers for hydrogen adsorption. *J. Colloid Interface Sci.* 318, 42-49.
- Im, J.S., Park, S.-J., Kim, T.J., Kim, Y.H. and Lee, Y.-S., 2008c. The study of controlling pore size on electrospun carbon nanofibers for hydrogen adsorption. *J. Colloid Interface Sci.* 318, 42-49.
- Im, J.S., Park, S.-J. and Lee, Y.-S., 2009b. The metal-carbon-fluorine system for improving hydrogen storage by using metal and fluoride with different levels of electronegativity. *Int. J. Hydro. Energy* 34, 1423-1428.
- Im, J.S., Park, S.-J. and Lee, Y.-S., 2009c. Superior prospect of chemically activated electrospun carbon fibers for hydrogen storage. *Mater. Res. Bull.* 44, 1871-1878.
- Jiang, Q., Qu, M.Z., Zhou, G.M., Zhang, B.L. and Yu, Z.L., 2002. A study of activated carbon nanotubes as electrochemical supercapacitors electrode materials. *Mater. Lett.* 57, 988-991.
- Jung, M.-J., Im, J.S., Jeong, E., Jin, J. and Lee, Y.-S., 2009. Hydrogen adsorption of PAN-based porous carbon nanofibers using MgO as the substrate. *Carbon Lett.* 10, 217-220.
- Jung, W.H., Kwak, N.-S., Hwang, T.S. and Yi, K.B., 2012. Preparation of highly porous TiO<sub>2</sub> nanofibers for dye-sensitized solar cells (DSSCs) by electro-spinning. *Appl. Surf. Sci.* 261, 343-352.
- Kim, B.-J., Lee, Y.-S. and Park, S.-J., 2007a. A study on pore-opening behaviors of graphite nanofibers by a chemical activation process. *J. Colloid Interface Sci.* 306, 454-458.
- Kim, B.-K., Park, S.H. and Kim, B.C., 2005. Electrospun polyacrylonitrile-based carbon nanofibers and their hydrogen storage. *Macromol. Res.* 13, 521-528.
- Kim, C.H., Kim, B.-H. and Yang, K.S., 2012. TiO<sub>2</sub> nanoparticles loaded on graphene/carbon composite nanofibers by electrospinning for increased photocatalysis. *Carbon* 50, 2472-2481.
- Kim, H., Lee, D. and Moon, J., 2011. Co-electrospun Pd-coated porous carbon nanofibers for hydrogen storage applications. *Int. J. Hydro. Energy* 36, 3566-3573.
- Kim, I.-D., Hong, J.-M., Lee, B.H., Kim, D.Y., Jeon, E.-K., Choi, D.-K. and Yang, D.-J., 2007b. Dye-sensitized solar cells using network structure of electrospun ZnO nanofiber mats. *Appl. Phys. Lett.* 91, 163109.
- Kim, J.-U., Park, S.-H., Choi, H.-J., Lee, W.-K., Lee, J.-K. and Kim, M.-R., 2009. Effect of electrolyte in electrospun poly(vinylidene fluoride-co-hexafluoropropylene) nanofibers on dye-sensitized solar cells. *Sol. Energy Mater. Sol. Cells* 93, 803-807.
- Kim, S., Kim, M., Kim, Y.K., Hwang, S.H. and Lim, S.K., 2014. Core-shell-structured carbon nanofiber-titanate nanotubes with enhanced photocatalytic activity. *Appl. Catal.*, B 148-149, 170-176.
- Kumar, P.S., Nizar, S.A.S., Sundaramurthy, J., Ragupathy, P., Thavasi, V., Mhaisalkar, S.G. and Ramakrishna, S., 2011. Tunable hierarchical TiO<sub>2</sub> nanostructures by controlled annealing of electrospun fibers: formation mechanism, morphology, crystallographic phase and photoelectrochemical performance analysis. *J. Mater. Chem.* 21, 9784.
- Kumar, P.S., Sahay, R., Aravindan, V., Sundaramurthy, J., Wong Chui, L., Thavasi, V., Mhaisalkar, S.G., Madhavi, S. and Seeram, R., 2012. Free-

- standing electrospun carbon nanofibres—a high performance anode material for lithium-ion batteries. *J. Phys. D: Appl. Phys.* 45, 265302.
- Kurban, Z., Lovell, A., Bennington, S.M., Jenkins, D.W.K., Ryan, K.R., Jones, M.O., Skipper, N.T. and David, W.I.F., 2010. A solution selection model for coaxial electrospinning and its application to nanostructured hydrogen storage materials. *J. Phys. Chem. C* 114, 21201-21213.
- Lakshmi, B.B., Patrissi, C.J. and Martin, C.R., 1997. Sol-Gel Template Synthesis of Semiconductor Oxide Micro- and Nanostructures. *Chem. Mater.* 9, 2544-2550.
- Law, M., Goldberger, J. and Yang, P., 2004. Semiconductor Nanowires and Nanotubes. *Annu. Rev. Mater. Res.* 34, 83-122.
- Lee, H.U., Park, S.Y., Lee, S.C., Seo, J.H., Son, B., Kim, H., Yun, H.J., Lee, G.W., Lee, S.M., Nam, B., Lee, J.W., Huh, Y.S., Jeon, C., Kim, H.J. and Lee, J., 2014. Highly photocatalytic performance of flexible 3 dimensional (3D) ZnO nanocomposite. *Appl. Catal. B* 144, 83-89.
- Lee, S.S., Bai, H., Liu, Z. and Sun, D.D., 2012. Electrospun TiO<sub>2</sub>/SnO<sub>2</sub> nanofibers with innovative structure and chemical properties for highly efficient photocatalytic H<sub>2</sub> generation. *Int. J. Hydro. Energy* 37, 10575-10584.
- Li, H., Zhang, W., Huang, S. and Pan, W., 2012a. Enhanced visible-light-driven photocatalysis of surface nitrated electrospun TiO<sub>2</sub> nanofibers. *Nanoscale* 4, 801-806.
- Li, J., Chen, X., Ai, N., Hao, J., Chen, Q., Strauf, S. and Shi, Y., 2011. Silver nanoparticle doped TiO<sub>2</sub> nanofiber dye sensitized solar cells. *Chem. Phys. Lett.* 514, 141-145.
- Li, Q., Chen, Y., Lee, D.J., Li, F. and Kim, H., 2012b. Preparation of Y-zeolite/CoCl<sub>2</sub> PVDF composite nanofibers and its application in hydrogen production. *Energy* 38, 144-150.
- Lin, Y.P., Chen, Y.Y., Lee, Y.C. and Chen-Yang, Y.W., 2012. Effect of wormhole-like mesoporous anatase TiO<sub>2</sub> nanofiber prepared by electrospinning with ionic liquid on dye-sensitized solar cells. *J. Phys. Chem. C* 116, 13003-13012.
- Liu, B. and Zeng, H.C., 2003. Hydrothermal synthesis of ZnO nanorods in the diameter regime of 50 nm. *J. Am. Chem. Soc.* 125, 4430-4431.
- Liu, C., Fan, Y.Y., Liu, M., Cong, H.T., Cheng, H.M. and Dresselhaus, M.S., 1999. Hydrogen storage in single-walled carbon nanotubes at room temperature. *Science* 286, 1127-1129.
- Ma, D., Xin, Y., Gao, M. and Wu, J., 2014. Fabrication and photocatalytic properties of cationic and anionic S-doped TiO<sub>2</sub> nanofibers by electrospinning. *Appl. Catal. B* 147, 49-57.
- Madhavan, A.A., Kumar, G.G., Kalluri, S., Joseph, J., Nagarajan, S., Nair, S., Subramanian, K.R.V. and Balakrishnan, A., 2012. Effect of embedded plasmonic Au nanoparticles on photocatalysis of electrospun TiO<sub>2</sub> nanofibers. *J. Nanosci. Nanotechnol.* 12, 7963-7967.
- Maiyalagan, T., Sundaramurthy, J., Kumar, P.S., Kannan, P., Opallo, M. and Ramakrishna, S., 2013. Nanostructured  $\alpha$ -Fe<sub>2</sub>O<sub>3</sub> platform for the electrochemical sensing of folic acid. *Analyst* 138, 1779-1786.
- Meng, X., Shin, D.-W., Yu, S.M., Jung, J.H., Kim, H.I., Lee, H.M., Han, Y.-H., Bhoraskar, V. and Yoo, J.-B., 2011. Growth of hierarchical TiO<sub>2</sub> nanostructures on anatase nanofibers and their application in photocatalytic activity. *CrystEngComm* 13, 3021.
- Mitani, S., Lee, S.-I., Saito, K., Yoon, S.-H., Korai, Y. and Mochida, I., 2005. Activation of coal tar derived needle coke with K<sub>2</sub>CO<sub>3</sub> into and active carbon of low surface area and its performance as unique electrode of electric double-layer capacitor. *Carbon* 43, 2960-2967.
- Nair, A.S., Jose, R., Shengyuan, Y. and Ramakrishna, S., 2011. A simple recipe for an efficient TiO<sub>2</sub> nanofiber-based dye-sensitized solar cell. *J. Colloid Interface Sci.* 353, 39-45.
- Nair, A.S., Zhu, P., Babu, V.J., Yang, S., Krishnamoorthy, T., Murugan, R., Peng, S. and Ramakrishna, S., 2012. TiO<sub>2</sub> derived by titanate route from electrospun nanostructures for high-performance dye-sensitized solar cells. *Langmuir* 28, 6202-6206.
- Neubert, S., Pliszka, D., Thavasi, V., Wintermantel, E. and Ramakrishna, S., 2011. Conductive electrospun PANi-PEO/TiO<sub>2</sub> fibrous membrane for photocatalysis. *Mater. Sci. Eng., B* 176, 640-646.
- Pant, B., Pant, H.R., Barakat, N.A.M., Park, M., Jeon, K., Choi, Y. and Kim, H.-Y., 2013. Carbon nanofibers decorated with binary semiconductor (TiO<sub>2</sub>/ZnO) nanocomposites for the effective removal of organic pollutants and the enhancement of antibacterial activities. *Ceram. Int.* 39, 7029-7035.
- Park, S.-H., Jung, H.-R., Kim, B.-K. and Lee, W.-J., 2012. MWCNT/mesoporous carbon nanofibers composites prepared by electrospinning and silica template as counter electrodes for dye-sensitized solar cells. *J. Photochem. Photobiol., A* 246, 45-49.
- Park, S.-H., Jung, H.-R. and Lee, W.-J., 2013. Hollow activated carbon nanofibers prepared by electrospinning as counter electrodes for dye-sensitized solar cells. *Electrochim. Acta* 102, 423-428.
- Park, S.-H., Won, D.-H., Choi, H.-J., Hwang, W.-P., Jang, S.-i., Kim, J.-H., Jeong, S.-H., Kim, J.-U., Lee, J.-K. and Kim, M.-R., 2011. Dye-sensitized solar cells based on electrospun polymer blends as electrolytes. *Sol. Energy Mater. Sol. Cells* 95, 296-300.
- Peining, Z., Nair, A.S., Shengjie, P., Shengyuan, Y. and Ramakrishna, S., 2012. Facile fabrication of TiO<sub>2</sub>-Graphene Composite with enhanced photovoltaic and photocatalytic properties by electrospinning. *ACS Appl. Mater. Inter.* 4, 581-585.
- Peng, S., Zhu, P., Wu, Y., Mhaisalkar, S.G. and Ramakrishna, S., 2012a. Electrospun conductive polyaniline-poly(lactic acid) composite nanofibers as counter electrodes for rigid and flexible dye-sensitized solar cells. *RSC Adv.* 2, 652.
- Peng, X., Santulli, A.C., Sutter, E. and Wong, S.S., 2012b. Fabrication and enhanced photocatalytic activity of inorganic core-shell nanofibers produced by coaxial electrospinning. *Chem. Sci.* 3, 1262-1272.
- Reardon, H., Hanlon, J.M., Hughes, R.W., Godula-Jopei, A., Mandal, T.K. and Gregory, D.H., 2012. Emerging concepts in solid-state hydrogen storage: the role of nanomaterials design. *Energy Environ. Sci.* 5, 5951.
- Rose, M., Kockrick, E., Senkovska, I. and Kaskel, S., 2010. High surface area carbide-derived carbon fibers produced by electrospinning of polycarbosilane precursors. *Carbon* 48, 403-407.
- Sahay, R., Kumar, P.S., Sridhar, R., Sundaramurthy, J., Venugopal, J., Mhaisalkar, S.G. and Ramakrishna, S., 2012a. Electrospun composite nanofibers and their multifaceted applications. *J. Mater. Chem.* 22, 12953.
- Sahay, R., Sundaramurthy, J., Suresh Kumar, P., Thavasi, V., Mhaisalkar, S.G. and Ramakrishna, S., 2012b. Synthesis and characterization of CuO nanofibers, and investigation for its suitability as blocking layer in ZnO NPs based dye sensitized solar cell and as photocatalyst in organic dye degradation. *J. Solid State Chem.* 186, 261-267.
- Samadi, M., Shivaee, H.A., Zanetti, M., Pourjavadi, A. and Moshfegh, A., 2012. Visible light photocatalytic activity of novel MWCNT-doped ZnO electrospun nanofibers. *J. Mol. Catal. A: Chem.* 359, 42-48.
- Seo, S.-J., Yun, S.-H., Woo, J.-J., Park, D.-W., Kang, M.-S., Hirsch, A. and Moon, S.-H., 2011. Preparation and characterization of quasi-solid-state electrolytes using a brominated poly(2,6-dimethyl-1,4-phenylene oxide) electrospun nanofiber mat for dye-sensitized solar cells. *Electrochem. Commun.* 13, 1391-1394.
- Shahgaldi, S., Yaakob, Z., Khadem, D.J. and Daud, W.R.W., 2012. Characterization and the hydrogen storage capacity of titania-coated electrospun boron nitride nanofibers. *Int. J. Hydro. Energy* 37, 11237-11243.
- Shengyuan, Y., Peining, Z., Nair, A.S. and Ramakrishna, S., 2011. Rice grain-shaped TiO<sub>2</sub> mesostructures-synthesis, characterization and applications in dye-sensitized solar cells and photocatalysis. *J. Mater. Chem.* 21, 6541-6548.
- Singh, P., Mondal, K. and Sharma, A., 2013. Reusable electrospun mesoporous ZnO nanofiber mats for photocatalytic degradation of polycyclic aromatic hydrocarbon dyes in wastewater. *J. Colloid Interface Sci.* 394, 208-215.
- Song, L., Du, P., Shao, X., Cao, H., Hui, Q. and Xiong, J., 2013a. Effects of hydrochloric acid treatment of TiO<sub>2</sub> nanoparticles/nanofibers bilayer film on the photovoltaic properties of dye-sensitized solar cells. *Mater. Res. Bull.* 48, 978-982.
- Song, L., Xiong, J., Jiang, Q., Du, P., Cao, H. and Shao, X., 2013b. Synthesis and photocatalytic properties of Zn<sup>2+</sup> doped anatase TiO<sub>2</sub> nanofibers. *Mater. Chem. Phys.* 142, 77-81.
- Song, M.Y., Kim, D.K., Jo, S.M. and Kim, D.Y., 2005. Enhancement of the photocurrent generation in dye-sensitized solar cell based on electrospun TiO<sub>2</sub> electrode by surface treatment. *Synth. Met.* 155, 635-638.
- Srinivasan, S.S., Ratnadurai, R., Niemann, M.U., Phani, A.R. and Goswami, D.Y., 2010. Reversible hydrogen storage in electrospun polyaniline fibers. *Int. J. Hydro. Energy* 35, 225-230.
- Su, Q., Zhang, J., Wang, Y., Yu, M., Zhu, C., Lan, W. and Liu, X., 2013. Effect of the morphology of V<sub>2</sub>O<sub>5</sub>/TiO<sub>2</sub> nanoheterostructures on the visible

- light photocatalytic activity. *J. Phys. Chem. Solids* 74, 1475-1481.
- Sun, X., Cheng, L., Zhu, W., Hu, C., Jin, R., Sun, B., Shi, Y., Zhang, Y. and Cui, W., 2014. Use of ginsenoside Rg3-loaded electrospun PLGA fibrous membranes as wound cover induces healing and inhibits hypertrophic scar formation of the skin. *Colloids Surf., B* 115, 61-70.
- Sundaramurthy, J., Kumar, P.S., Kalaivani, M., Thavasi, V., Mhaisalkar, S.G. and Ramakrishna, S., 2012. Superior photocatalytic behaviour of novel 1D nanobraid and nanoporous  $\alpha$ -Fe<sub>2</sub>O<sub>3</sub> structures. *RSC Adv.* 2, 8201-8208.
- Szilágyi, I.M., Santala, E., Heikkilä, M., Pore, V., Kemell, M., Nikitin, T., Teucher, G., Firkala, T., Khriachtchev, L., Räsänen, M., Ritala, M. and Leskelä, M., 2013. Photocatalytic Properties of WO<sub>3</sub>/TiO<sub>2</sub> core/shell nanofibers prepared by electrospinning and atomic layer deposition. *Chem. Vap. Deposition* 19, 149-155.
- Teoh, W.Y., Scott, J.A. and Amal, R., 2012. Progress in heterogeneous photocatalysis: from classical radical chemistry to engineering nanomaterials and solar reactors. *J. Phys. Chem. Lett.* 3, 629-639.
- Thavasi, V., Renugopalakrishnan, V., Jose, R. and Ramakrishna, S., 2009. Controlled electron injection and transport at materials interfaces in dye sensitized solar cells. *Mater. Sci. Eng., R: Reports* 63, 81-99.
- Tsuchiya, H. and Schmuki, P., 2005. Self-organized high aspect ratio porous hafnium oxide prepared by electrochemical anodization. *Electrochem. Commun.* 7, 49-52.
- Xue, R., Behera, P., Xu, J., Viapiano, M.S. and Lannutti, J.J., 2014. Polydimethylsiloxane core-polycaprolactone shell nanofibers as biocompatible, real-time oxygen sensors. *Sens. Actuators, B* 192, 697-707.
- Yaakob, Z., Khadem, D.J., Shahgaldi, S., Daud, W.R.W. and Tasirin, S.M., 2012. The role of Al and Mg in the hydrogen storage of electrospun ZnO nanofibers. *Int. J. Hydro. Energy* 37, 8388-8394.
- Yang, J.L., An, S.J., Park, W.I., Yi, G.C. and Choi, W., 2004. Photocatalysis using ZnO thin films and nanoneedles grown by metal-organic chemical vapor deposition. *Adv. Mater.* 16, 1661-1664.
- Yousef, A., Barakat, N.A.M., Al-Deyab, S.S., Nirmala, R., Pant, B. and Kim, H.Y., 2012a. Encapsulation of CdO/ZnO NPs in PU electrospun nanofibers as novel strategy for effective immobilization of the photocatalysts. *Colloids Surf., A* 401, 8-16.
- Yousef, A., Barakat, N.A.M., Khalil, K.A., Unnithan, A.R., Panthi, G., Pant, B. and Kim, H.Y., 2012b. Photocatalytic release of hydrogen from ammonia borane-complex using Ni (0)-doped TiO<sub>2</sub>/C electrospun nanofibers. *Colloids Surf., A* 410, 59-65.
- Yousef, A., Barakat, N.A.M. and Kim, H.Y., 2013. Electrospun Cu-doped titania nanofibers for photocatalytic hydrolysis of ammonia borane. *Appl. Catal., A* 467, 98-106.
- Yuan, Y., Zhao, Y., Li, H., Li, Y., Gao, X., Zheng, C. and Zhang, J., 2012. Electrospun metal oxide-TiO<sub>2</sub> nanofibers for elemental mercury removal from flue gas. *J. Hazard. Mater.* 227-228, 427-435.
- Yun, S. and Lim, S., 2011. Improved conversion efficiency in dye-sensitized solar cells based on electrospun Al-doped ZnO nanofiber electrodes prepared by seed layer treatment. *J. Solid State Chem.* 184, 273-279.
- Zhang, P., Shao, C., Li, X., Zhang, M., Zhang, X., Sun, Y. and Liu, Y., 2012a. In situ assembly of well-dispersed Au nanoparticles on TiO<sub>2</sub>/ZnO nanofibers: A three-way synergistic heterostructure with enhanced photocatalytic activity. *J. Hazard. Mater.* 237-238, 331-338.
- Zhang, W., Zhu, R., Liu, X., Liu, B. and Ramakrishna, S., 2009. Facile construction of nanofibrous ZnO photoelectrode for dye-sensitized solar cell applications. *Appl. Phys. Lett.* 95, 043304.
- Zhang, X., Thavasi, V., Mhaisalkar, S.G. and Ramakrishna, S., 2012b. Novel hollow mesoporous 1D TiO<sub>2</sub> nanofibers as photovoltaic and photocatalytic materials. *Nanoscale* 4, 1707-1716.
- Zhu, C., Li, Y., Su, Q., Lu, B., Pan, J., Zhang, J., Xie, E. and Lan, W., 2013. Electrospinning direct preparation of SnO<sub>2</sub>/Fe<sub>2</sub>O<sub>3</sub> heterojunction nanotubes as an efficient visible-light photocatalyst. *J. Alloys Compd.* 575, 333-338.